

Uncatalyzed aerobic epoxidation of liquid alkyl alkenes

Received: 1 March 2025

Accepted: 25 June 2025

Published online: 16 July 2025



Susi Hervàs-Arnandis^{1,2}, Francisco Garnes-Portolés^{1,2},
Silvia Rodríguez-Nuévalos¹, Judit Oliver-Meseguer¹✉ &
Antonio Leyva-Pérez¹✉

Researchers have investigated for decades a suitable catalyst to selectively synthesize epoxides from alkenes with air. Here we show that a selective aerobic epoxidation of industrial alkyl alkenes in liquid phase occurs without any catalyst, solvent nor additive, just placing the neat alkene under 3–5 bar of O₂ and heating between 100 and 200 °C. The reaction can be performed in either an autoclave, a stirring vessel with air bubbling or even a simple open flask, provided that any metal piece is not in contact with the reaction. Alkyl epoxides are directly obtained, after air venting, in yields and selectivity up to 90%. The simplicity of the set-up (just the neat liquid alkene and air) allows to engage the epoxidation reaction with either a previous alkene formation (upstreaming) or a later epoxide opening (downstreaming) reactions, to achieve a variety of industrially-relevant organic products in one-pot.

Alkyl epoxides are fundamental organic molecules in industry, with widespread application in our society on a daily basis, from surfactants to construction, electronics or adhesives, to name a few¹. Indeed, technological evolution cannot be understood without alkyl epoxides. The global alkyl epoxide market has been valued in ~€70 billion in 2024 and is expected to achieve >€90 billion in 2028, with a compound annual growth rate (CAGR) between 3 and 6% (<https://www.databridgemarketresearch.com/reports/global-epoxides-market>), (<https://www.thebusinessresearchcompany.com/report/epoxide-global-market-report>), which implies that megaton amounts of these epoxides are to be manufactured.

Figure 1A shows that the production of alkyl epoxides relies on the so-called epoxidation reaction of alkenes, which employs toxic, dangerous and relatively expensive oxidant agents such as water peroxide (H₂O₂), organic peroxides and hydroperoxides, in the presence of catalysts and with organic solvents for most of the processes except one, i.e., the epoxidation reaction of ethylene, which is carried out with molecular oxygen (O₂/air) over a Ag-supported catalyst at >500 °C². Therefore, it is not surprising that a long-sought reaction in synthetic chemistry is a general epoxidation reaction of alkenes with air^{3–7}. For that, a plethora of catalysts, most of them based on metals⁸, have been studied, in many cases with the

assistance of organic molecules able to shuttle the activated oxygen species to the alkene, such as aldehydes, ketones, or carboxylic acids^{9–11}. However, none of the systems found to date is apparently suitable to achieve the efficiency of the catalysed processes with H₂O₂ or organic peroxides/hydroperoxides.

Figure 1B depicts the reaction conditions traditionally employed during the epoxidation reaction of alkenes with air, catalyzed or not. It can be seen that, in general, O₂ pressures above 5 bar (>50 bar in many cases) are set over dissolved alkenes at high reaction temperatures¹². These conditions make sense if one considers the reluctance of O₂ to form the required electrophilic O atoms and react with the alkene to the target epoxide, and the expected increase in the extent of undesired alkene by-reactions at high concentrations (oligomerization, overoxidation...). Unfortunately, yields and selectivity to the desired epoxides are usually below 30%, and these precedents only highlight the uniqueness of ethylene to selectively react with O₂, due to its small size and the lack of any highly reactive allylic H atom. However, after a deep analysis of the literature, it seems that reaction conditions consisting in low O₂ pressures (<5 bar) and highly concentrated alkene solutions, even with the neat alkene, have been barely explored^{13,14}. These counterintuitive experimental reaction conditions are in turn those required by industry, where the

¹Instituto de Tecnología Química (Universitat Politècnica de València– Agencia Estatal Consejo Superior de Investigaciones Científicas), València, Spain.

²These authors contributed equally: Susi Hervàs-Arnandis, Francisco Garnes-Portolés. ✉ e-mail: joliverm@itq.upv.es; anleyva@itq.upv.es

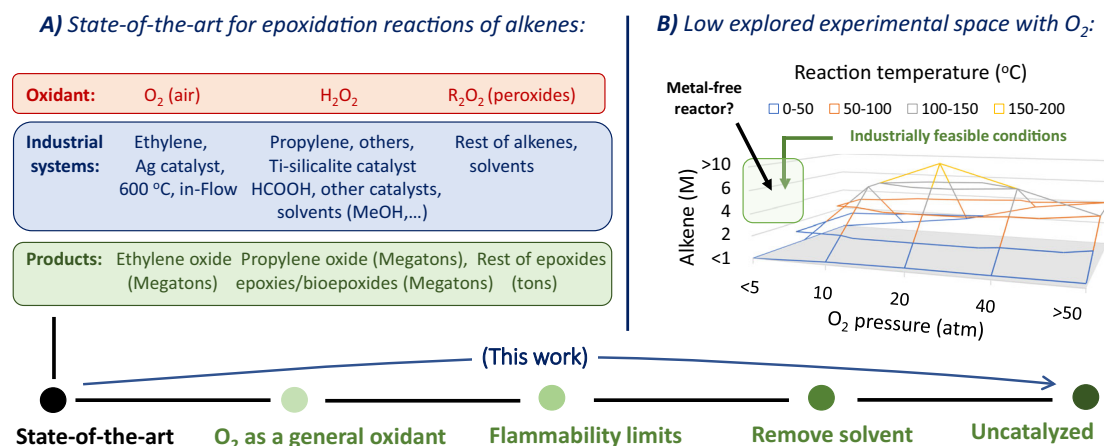


Fig. 1 | The challenge of a general and uncatalyzed aerobic epoxidation of alkenes. **A** State of the art for the epoxidation reaction of alkenes, with the different oxidants, industrial systems and epoxide products. **B** The typical reaction conditions in the literature for the aerobic epoxidation of alkenes, where the most feasible industrial conditions (diluted air, concentrated alkene) are little explored (this

Figure can be considered as a cartoon of the state-of-the-art rather than a quantitative calculation of the different reports). Bottom: The step forward of the results presented here, from unsatisfactory catalysed processes under flammable conditions with organic solvents to the here reported uncatalyzed, solventless process within flammability limits.

flammability limits of the alkyl alkenes severely decrease the partial O_2 pressure allowed during reaction¹³, and where reactor occupancy must be maximized to increase the reaction throughput. Another important factor to be considered here is the use of metal reactors, majorly used in previous studies despite metals tend to uncontrollably decompose O_2 into very reactive species, which unavoidably over-oxidize the alkene and epoxide to ketones and carboxylic acids^{14–16}.

Here we show that a variety of alkyl alkenes are transformed to the corresponding epoxides in high yields and selectivity when reacting in neat form with O_2 , at pressures below 5 bar and without metal pieces in the reactor. Regardless the auto-oxidation of alkenes, especially for aryl alkenes and cyclic alkenes, has been known for decades with peroxides^{17–20}, a comprehensive previous study focused on the aerobic selective epoxidation reaction has not been performed as far as we know, in the absence of peroxyradicals^{21,22}. Any catalyst, solvent nor additive is not required, just the alkene and O_2 , which allows to obtain the epoxide product directly after O_2 venting, and to start a subsequent reaction on the epoxide if required. Complementarily, the alkene can be previously formed by conventional reactions such as isomerization²³ or alkene metathesis, and then epoxidized in one-pot with just O_2 , and the epoxide product further elaborated, in-situ²⁴. The epoxidation reaction can be run not only in autoclaves but also in regular glass flasks with TeflonTM-coated magnetic stirs under air-bubbling or open-flask conditions. The bottom of Fig. 1 depicts the step forward that, in our opinion, our results constitute in the field of epoxidation reactions. These results might be seen as a practical outcome of more than 75 years of research in the direct oxidation of alkenes with air. In the 50's, several works introduced the notion of direct reaction of alkenes with O_2 to give the epoxide vs. the more common allylic hydrogen removal, to give the alternative hydroperoxide²⁵. During the next three decades, the concept was expanded with more examples²⁶ and with new insights into the reaction mechanism, presenting alkene cation radicals and peroxides as potential intermediate species^{12,27}. However, the irruption of metal catalysts for the allylic hydrogen abstraction reaction to generate hydroperoxide intermediates²⁸ and the lack of practical examples for a direct aerobic epoxidation beyond cyclooctene²⁹ apparently diminished the interest for studying the direct epoxidation of alkenes.

Results

Optimization of the reaction conditions: from autoclaves to open flask reactors

We found by serendipity that the reaction between neat alkenes and O_2 occurs in significant extent under mild reaction conditions, at low O_2 pressures. Suprun and Opeida described the oxidation of styrene in the cumene solution²⁰, and that could be the first time when it was observed, experimentally, the epoxidation without solvent and O_2 as the epoxidation agent. Our attempts to reproduce some catalytic results for the epoxidation of styrene **1a** under 4 bar of O_2 lead us to the conclusion that neither the metal catalyst nor the solvent were required to convert the alkene, after following the reaction by gas chromatography coupled to mass spectrometry (GC–MS, see Fig. S1 in Supplementary Information). Indeed, the conversion of styrene was higher in the absence of any catalyst and solvent (compare entries 1, 5, and 7 in Table S1). The reactions were run in glass autoclaves with a TeflonTM-coated magnetic bar, which in principle discards any O_2 activation by a metal. Despite the selectivity to styrene epoxide was not good in the absence of *N,N*-dimethylformamide, which can exert here as an O_2 activator (aldehyde), we studied the possible epoxidation reaction of other alkenes under solventless reaction conditions and 4 bar of O_2 , and Fig. 2A shows the results with a variety of liquid alkyl and cyclic alkenes. The secondary alkyl alkene 7-tetradecene **1b** (*trans/cis* 75:25) gives the corresponding *trans*-isomer enriched epoxide **2b** in 74% yield after complete conversion of the starting material (18 h reaction time), tripled checked by GC–MS, ¹H nuclear magnetic resonance (¹H NMR) and isolated yield after purification by flash column chromatography (averaged yield). The rest of products mainly correspond to overoxidized products, such as aldehydes, carboxylic acids and alcohols. As the alkyl chains flanking the secondary alkene shorten, the selectivity and yield to the epoxide product decrease, and 3-octene **1c** (pure *trans*) and 4-octene **1d** (pure *trans*) give epoxides **2c** and **2d** in 54/40% and 16/16% selectivity/yield, respectively. The terminal alkene 1-tetradecene **1e** was completely unreactive during reaction under similar reaction conditions. The cyclic alkenes cyclododecene **1f** (*cis/trans* 73:25), cyclooctene **1g** (pure *cis*) and cyclohexene **1h** (pure *cis*) followed the same trend³⁰ than the open chain alkyl alkenes, i.e., the longer the alkyl chain the higher the yield to the epoxide product, to give epoxides **2f**, **2g** and **2h** in 93/77%, 84/79% and 4/4% selectivity/yield, respectively. These results indicate that secondary alkenes with relatively long alkyl chains, typically more than six carbon atoms,

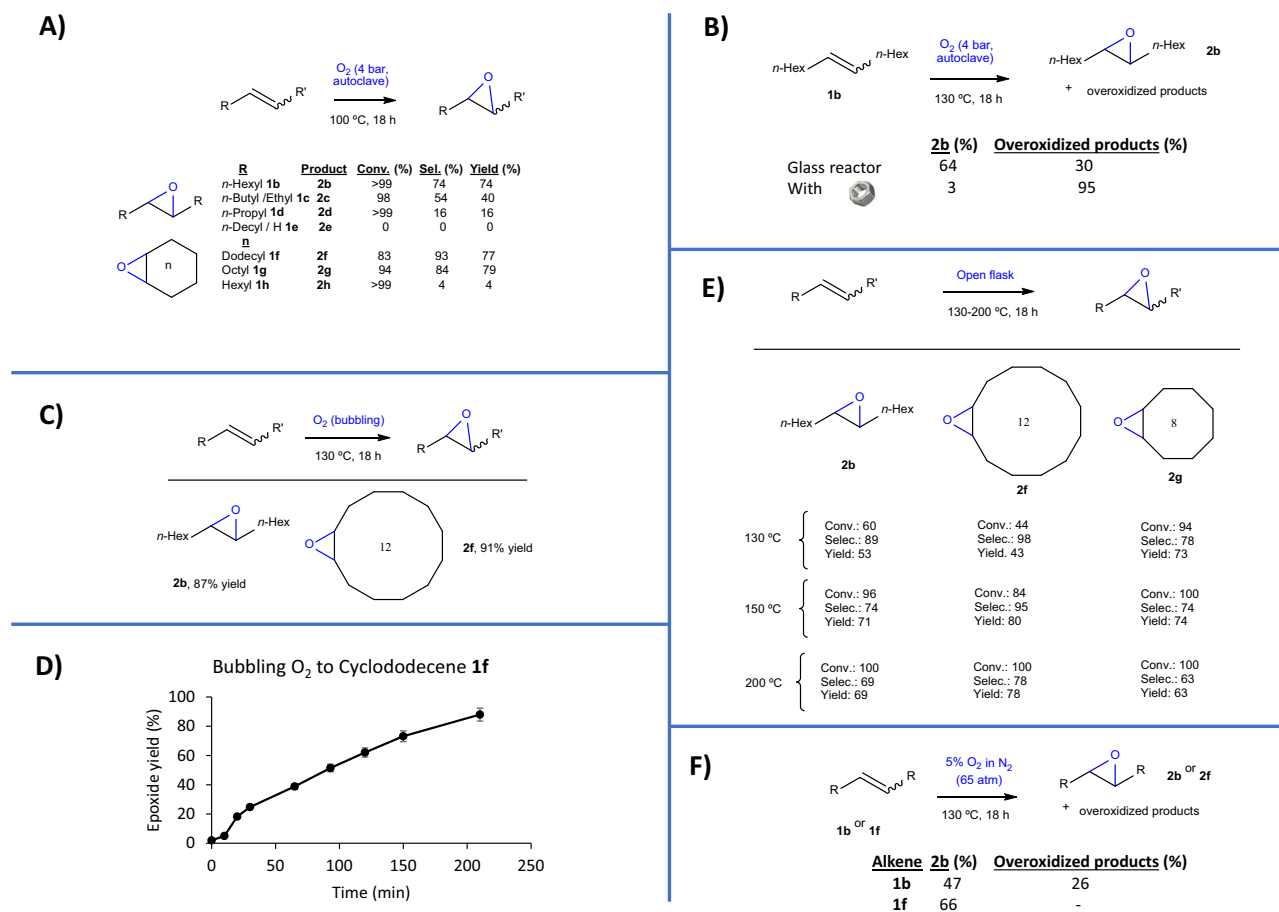


Fig. 2 | Optimization of the reaction conditions for the uncatalyzed aerobic epoxidation reaction of alkenes. **A** Results for the epoxidation reaction of alkenes **1b–h** under 4 bar of O₂ in a glass autoclave reactor at 100 °C for 18 h. **B** Results for the epoxidation reaction of alkene **1b** at 130 °C under the reaction conditions of (**A**) and in the presence or not of a metal nut. **C** Results for the epoxidation reaction of alkenes **1b** and **1f** after bubbling O₂ through the neat alkene at 130 °C for 18 h. **D** Kinetic plot for the epoxidation reaction of alkene **1f** in a round-bottomed flask

with O₂ bubbling at 200 °C. **E** Results for the epoxidation reaction of alkenes **1b**, **1f**, and **1g** under reaction conditions in (**D**) (open flask) at different temperatures. **F** Results for the epoxidation reaction of alkenes **1b** and **1f** under 65 bar of diluted (5%) O₂ in N₂, in a Teflon™ vessel within an autoclave reactor at 130 °C for 18 h. All results refer to gas chromatography (GC) yields, triple checked mass spectrometry (GC-MS), ¹H nuclear magnetic resonance (¹H NMR), and isolated yield after purification by flash column chromatography.

convert to the corresponding epoxide products in good yields under 4 bar of O₂ at 100 °C.

Figure 2B shows that a higher reaction temperature (130 °C) does not produce an increase in the yield but a decrease in selectivity for 7-tetradecene **1b**, to give epoxide **2b** in 64% yield. At this point, we tried a wide scope for the reaction by using a steel multi-reactor autoclave at 100 °C under 4 bar of O₂, but all the alkene substrates tested, which included **1b–h**, only yielded overoxidized products, mainly carboxylic acids (results not shown). It is noteworthy that the terminal alkene 1-tetradecene **1e**, unreactive in the glass reactor, also decomposed to overoxidized products in the steel reactor. To check if the metal reactor was the cause of the overoxidation products, the epoxidation reaction in the glass reactor was repeated with a small metal nut inside the reaction mixture. As it can be seen in Fig. 2B, the yield of epoxide **2b** decreased to just 3% (compared to 64% without the metal nut) for a complete conversion of the starting material, the rest being overoxidation products, and when the reaction was repeated again with another metal nut previously passivated with diluted HNO₃, the yield of epoxide **2b** was restored. These results strongly suggest that the presence of non-passivated metal parts during the aerobic epoxidation reaction leads to overoxidation products and that either glass or properly passivated metal reactors must be used to maximize the epoxide products.

The epoxidation reaction of alkenes 7-tetradecene **1b** and cyclododecene **1f** was then tested in a round-bottomed flask reaction after bubbling O₂ through the neat alkene, at 130 °C (Fig. S2). The results in Fig. 2C shows that the epoxide products **2b** and **2f** were obtained in very high yields (87–91%) after 18 h reaction time and the kinetic plot in Fig. 2D shows that the yield of epoxide **2f** reaches 90% after just 3.5 h reaction time. Then, we tested the epoxidation reaction in an open round-bottomed flask, just connecting a reflux condenser in order to avoid any loss of alkene. The reaction temperature was set at 200 °C in the thought that the relatively low concentration of O₂ in the atmosphere will severely decrease the epoxidation reaction rate, however, this was not the case, since Fig. 2E shows that the optimal reaction temperature under open flask conditions is 150 °C, with yields between 70–80% for the different alkenes tested. A kinetic experiment shows the smooth formation of the epoxide product (Fig. S3). At lower reaction temperatures, the reactions may stop at moderate conversions (40–60%) because of the higher density of the incipient epoxide product, which hampers a suitable diffusion of O₂. However, the decomposition of the epoxide at this temperature could also play a role, although we did not observe much overoxidized products (which in any case would need a good O₂ mass transfer). To solve this problem, different solvents were employed, and *n*-dodecane and toluene showed to be compatible with the epoxidation reaction, to give epoxide **2b** in high yields in concentrated solutions (7.8 M, Table S2).

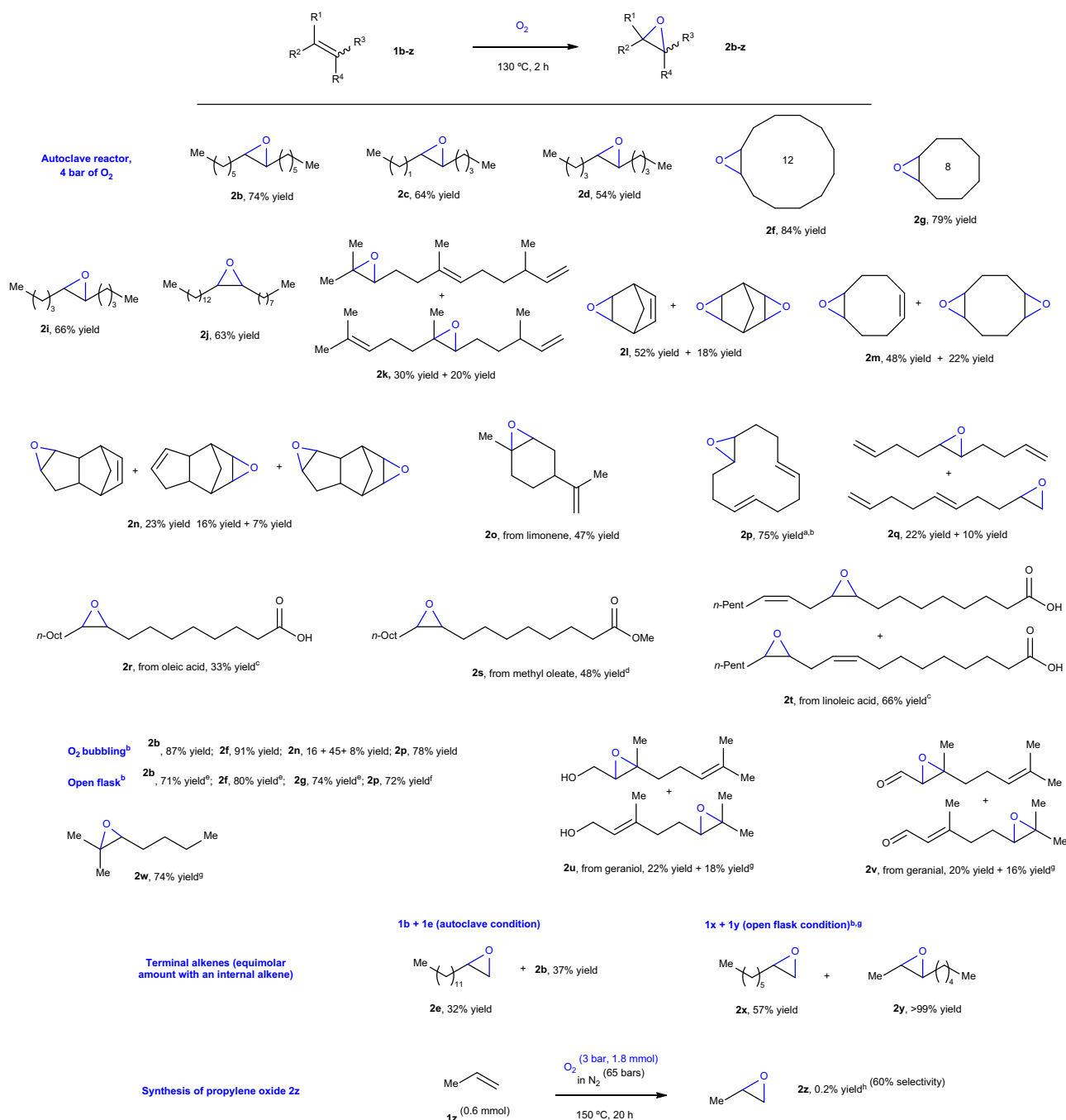


Fig. 3 | Scope of the uncatalyzed aerobic epoxidation reaction of alkenes.

Results for the epoxidation reaction of alkenes **1b–z** either under glass autoclave reactors (4 bar of O₂), bubbling of O₂ through the neat alkene or open flask reaction

conditions, under the indicated reaction conditions. Isolated yields. ^a 45% yield with O₂ diluted in N₂ (5% in 65 bar). ^b 18 h reaction time. ^c 30 min reaction time. ^d 3 h reaction time. ^e 150 °C. ^f 200 °C. ^g 100 °C. ^h ¹H NMR combined with GC–MS yield.

but not in diluted conditions (compare entries 2–5). Other solvents, such as DMF, are not suitable for the aerobic epoxidation reaction (entry 6).

In view that the epoxidation reaction proceeds in a diluted O₂ atmosphere, such as ambient pressure, the reaction was carried out with diluted (5%) O₂ in N₂, which is a typical allowed reaction atmosphere in industry for highly flammable substances. A 65 bar total gauge pressure was set to achieve a similar O₂ partial pressure (~3 bar) than in previous experiments. The epoxidation reactions of alkenes **1b** and **1f** were performed in TeflonTM vessels within metal autoclave reactors at 130 °C for 18 h, and the results in Fig. 2F show that a yield/selectivity value of 47/64% for epoxide **2b** and 66/>99%

for epoxide **2f** were obtained. Slight variations in the reaction temperature and O₂ dilution improve the yield and selectivity for the epoxide products (Table S3). These results, together, confirm that the selective epoxidation of secondary alkenes can be performed in either autoclave reactors with 3–4 bar O₂ partial pressures (including industrially feasible O₂/N₂ mixtures) and round-bottomed flasks after bubbling O₂ or just opening the flask, with high yields of the corresponding epoxide products, and with the possibility of adding small amount of *n*-dodecane or toluene to better handling the reaction mixture³¹. Notice that all these reaction conditions are in principle, implementable under industrial environments but also practical at the laboratory scale. Indeed, since we do not have any catalyst, the

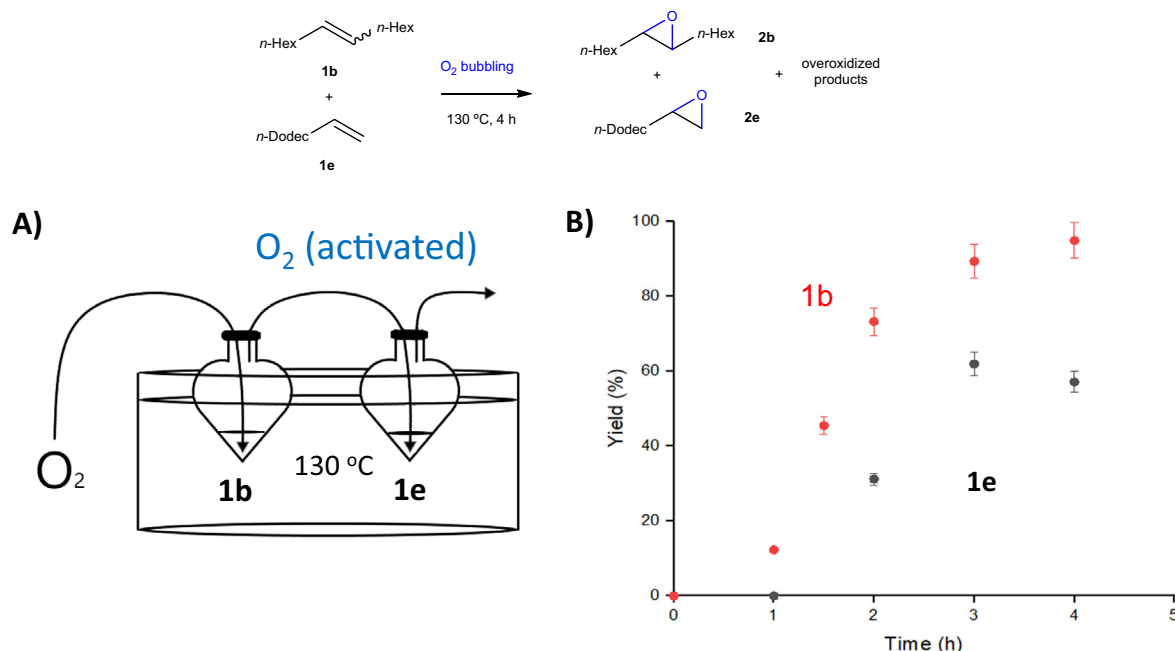


Fig. 4 | Two-pots epoxidation experiment. **A** Schematic representation of the two-pot experiment where O_2 is bubbled in a first flask with the internal alkene **1b** and the gas exit is connected to a second flask with the terminal alkene **1e**. **B** Kinetic

plots for the epoxidation reactions of alkenes **1b** and **1e** in the two-pots epoxidation experiment.

productivity only depends of the scale of the reaction, and for a 10-g reaction with 90% yield (see for instance Fig. S2), the productivity after 4 h would be $\approx 2 \text{ g}\cdot\text{h}^{-1}$, and if scaled up to 10 Kg (which is plausible considering that any other additive or solvent is not employed, apart of the alkene substrate), the productivity after 4 h would be $\approx 2 \text{ Kg}\cdot\text{h}^{-1}$. These numbers might be attractive from an industrial point of view.

Scope of the reaction conditions

Figure 3 shows the results for the uncatalyzed and solventless aerobic epoxidation reaction of a variety of alkenes either in glass autoclave reactors under 4 bar of O_2 , or round-bottomed flasks with bubbling O_2 or open reaction conditions. The results show that the three conditions can be employed with similar results (compare products **2b**, **2f**, **2g**, **2n**, and **2p**). The reaction time for the glass autoclave reactors can be diminished to just a couple of hours or even to 30 min. Open and cyclic alkyl chain secondary alkenes of different sizes react well to give the epoxides in moderate to very good isolated yields (products **2b–k**, 50–84%). The epoxide product is very stable under reaction conditions since purified product **2b** stays unchanged for 3 h under the O_2 pressure (5 bar) at 130 °C. Secondary dienes are also reactive, including bridged cycles, to give the corresponding mixture of mono- and di-epoxides in good combined yields (products **2l–n**, 46–70%). Remarkably, a diene such as limonene **1o**, where one of the alkenes is terminal (geminal) and the other is internal and tertiary, reacts exclusively through the internal alkene to give the industrially relevant limonene epoxide **2o** in 47% yield. Trienes also selectively react by one of the alkenes, and *all-trans* cyclododecatriene **1p** gives the monoepoxide **2p** in a consistent 72–78% isolated yield with the three reaction methodologies, i.e., pressure, bubbling or open flask. It is worthy remarking here that **1p** and its different *cis/trans* isomers constitutes the starting point to all macrocycles in the market, since the former is manufactured by trimerization of isobutene and gives access to cyclododecanone. Thus, the monoepoxide **2p** here formed, with three different functional groups handles, can be used as an alternative precursor for the macrocycle market. The reaction under O_2 diluted in

N_2 (5% in a total pressure of 65 bar) gave a 45% yield after 18 h reaction time (Fig. S4B).

Triene **1q**, with two terminal alkenes and one internal secondary alkene, reacted through the two alkenes (product **2q**, 22% internal + 10% terminal alkene), which may indicate that a terminal alkene becomes reactive in the presence of an internal alkene. To test this hypothesis, the epoxidation reaction of a mixture 1-tetradecene **1e** and 7-tetradecene **1b** was carried out, and Fig. 3 shows that the unreactive terminal alkene gives a 32% yield of the corresponding epoxide **2e**. At this point, a two-pot epoxidation experiment was designed, as shown in Fig. 4. In this set-up, O_2 is bubbled in a first flask containing the internal alkene **1b** and the gas exit is connected to a second flask containing the terminal alkene **1e**, both at 130 °C but not in contact. The kinetic plots show that the unreactive terminal alkene **1e** converts to the epoxide **2e** in >60% yield after the gas coming from the first flask (with the internal alkene **1b**) is passed through; in other words, that the O_2 gas passing through alkene **1b** is active to epoxidize terminal alkene **1e**. These results would be further commented in the mechanistic section. When we performed the reaction in the same pot, we obtained a similar result, i.e., a 32% yield of the epoxide **2e** together with a 40% yield of **2b** (Scheme 1).

Bio-based epoxides constitute a rocketing growing market, in particular from fatty acids derivatives to be employed in the adhesive and construction industry^{32,33}. Under our aerobic reaction conditions, oleic acid **1r**, methyl oleate **1s** and linoleic acid **1t** react to give the corresponding epoxides **2r–t** in 33–66% yield after just 30 min reaction time, according to optimized results (Table S4). Other diene natural products, such as geraniol **1u** and geranial **1v** react under open flask conditions to give the mixture of tri- and tetra-substituted epoxides **2u** and **2v** in ~40% combined yield, and the latter demonstrates that aldehyde groups are significantly compatible under these reaction conditions. The tri-substituted alkene **1w** gives a 74% yield of the quaternary epoxide **2w**. The open flask reaction conditions also allow the synthesis of terminal epoxides when combined with internal ones, as shown above, in this case the epoxide from 1-octene **1x** was obtained in 57% yield (product **2x**) concomitantly with the epoxide of

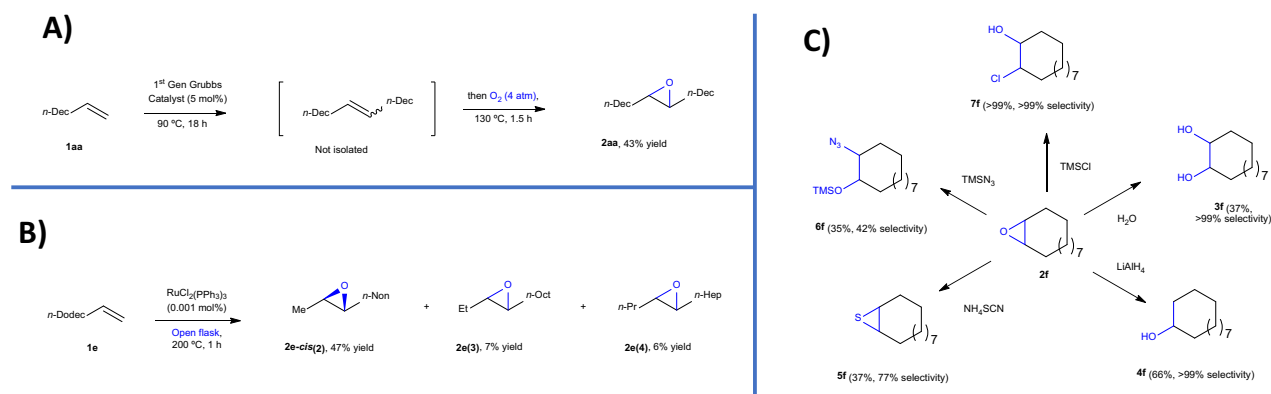


Fig. 5 | One-pot reactions. A Results for the one-pot, two-steps alkene metathesis-aerobic oxidation reaction with terminal alkene **1aa**. **B** Results for the one-pot alkene isomerization-aerobic oxidation tandem reaction with terminal alkene **1e**.

C Results for different reactions of the in-situ formed epoxide **2f** after uncatalyzed aerobic epoxidation reaction. The conversions obtained are given in brackets (see SI for more information about the procedures).

2-octene **1y** (>99% yield, product **2y**) at just 100 °C reaction temperature (see Fig. S5 for ¹H NMR spectra).

The aforementioned results demonstrate that, essentially, any sort of alkyl alkene, from terminal to highly substituted and from open to cyclic chains, can engage in the uncatalyzed solventless aerobic epoxidation reaction. In view of this, the reactivity of propylene **1z** was tested. Propylene oxide **2z** is, after ethylene epoxide, the highest epoxide industrially produced, despite peroxides must be employed during the catalytic fabrication process. With this in mind, we directly tested reaction conditions compatible with an industrial production of propylene oxide **2z** with O₂, i.e., diluted air and no additional additives nor alkenes and propylene in liquid conditions by increasing pressure. The result at the bottom of Fig. 3 shows that a 0.2% yield of neat **2z** (60% selectivity) could be obtained, according to ¹H NMR and GC–MS analysis under supercritical reaction conditions (70 bar and 150 °C, Fig. S6). The other 40% was the corresponding diol (glycol). Under liquid conditions (40 bar and 100 °C), any reactivity was not found. This yield for propylene oxide **2z** is in line with the low reactivity of terminal alkenes under reaction conditions. We have also tried an in-flow reaction with a tubular reactor for liquid substrates, after feeding air continuously at counter-gravity to a flow of 7-tetradecene **1b** (Fig. S7). However, we were not able to obtain a relevant conversion to the epoxide since it is much more difficult with this set-up to control the O₂/alkene dissolution rate respect to the batch conditions, leading to some amounts of overoxidation products even at low conversion.

One-pot reactions

The absence of any additional molecule, i.e., catalyst, oxidant, solvent, or additive, in the reaction mixture beyond the starting alkene and the epoxide product, invites to telescope the synthetic procedure, either upstream (formation of the alkene)³⁴ or downstream (transformation of the epoxide). Figure 5 shows the results obtained here. The classical alkene metathesis reaction³⁵ can be successfully combined with the aerobic epoxidation reaction to give the rare 2,3-bisdecyloxirane (10,11-*oxi-n*-docosane epoxide) product **2aa** in 43% yield from terminal alkene 1-dodecene **1aa** (Fig. 5A). O₂ cannot be present during the room temperature metathesis reaction since the 1st generation Grubbs catalyst (1st Gen Grubbs) would be decomposed, however, the catalyst and the dichloromethane solvent do not need to be removed after reaction, since O₂ can be directly charged in the reactor to give the epoxide product **2aa** after heating. However, a single-step protocol for the synthesis of internal epoxides from terminal alkenes would be in principle feasible since internal alkenes react with O₂ much faster than terminal alkenes according to the above results. Thus, we changed the

one-pot, two-step alkene metathesis-aerobic oxidation by a one-step alkene isomerization-aerobic oxidation reaction protocol, to generate an internal alkene by a simpler Ru catalyst, more tolerant to O₂ than the Grubbs catalyst (Fig. 5B)³⁶. The results with 1-tetradecene **1e** as the starting alkene show that not only the internal epoxide product **2e** is formed in good yield (~60%) but that the major product is the diastereo- and regio-isomerically defined product *cis*-2-methyl-3-undecyloxirane **2e-cis** (47% yield, 60% selectivity, see kinetics in Fig. S8). This product comes from the rapid quenching of the so-formed *cis* 2-tetradecene by O₂, which does not allow to generate significant amounts of neither the *trans* or the more internal alkenes, in an example of precise tandem reaction.

Regarding the downstream one-pot approach, the results for different reactions of the in-situ formed epoxide **2f** (after the uncatalyzed aerobic epoxidation reaction, yield 79% and selectivity 85%), are shown in Fig. 5C. It can be seen that epoxide **2f** was able to transform to different derivatives in the same reaction vessel. For instance, opening with H₂O led to glycol **3f** in 37% yield and complete selectivity, while reduction with LiAlH₄ gave cyclododecanol **4f** in 66% yield and also with complete selectivity. Less selective were the addition reactions with NH₄SCN and TMSN₃ (TMS is trimethylsilyl), which gave the thiirane **5f** and the silyl-protected azide **6f** products in 37/77% and 34/42% yield/selectivity, respectively. However, the addition of TMSCl gave the chloroalcohol **7f** quantitatively. The *cis* diastereoisomer reacted noticeably faster than the *anti* epoxide during these reactions, which was checked by kinetic experiments where the rapid consumption of the *cis* isomer was observed. Additionally, all these reactions were repeated with a simulated epoxidation reaction mixture using the commercial alkene **1f** and epoxide **2f**, and the reactions took place similarly, although in 5–10% less extent in some cases. We attribute the slight improvement in the one-pot reactions, with the in-situ formed epoxide, to the generation of some amounts of carboxylic acids as by-products, which can catalyze the epoxide opening reactions.

Reaction mechanism

The rate equation for the aerobic epoxidation reaction was determined by the pseudo-stationary method, measuring the initial rates for reactions where the concentration of one of the reactants, i.e., alkene **1b** and O₂, was varied. The concentration of O₂ was supposed to be linear with the pressure³⁷. The kinetic results for alkene **1b** (Fig. S9) and O₂ (Fig. S10) show that the equation rate fits to $v_0 = k_{\text{exp}}[\mathbf{1b}][\text{O}_2]$, where the two reactants behave with order +1, regardless if a solvent is employed (Fig. S9). These results indicate that one molecule of each reactant participates during the turnover-determining step (tds) of the reaction. Further kinetic experiments enable to calculate the activation

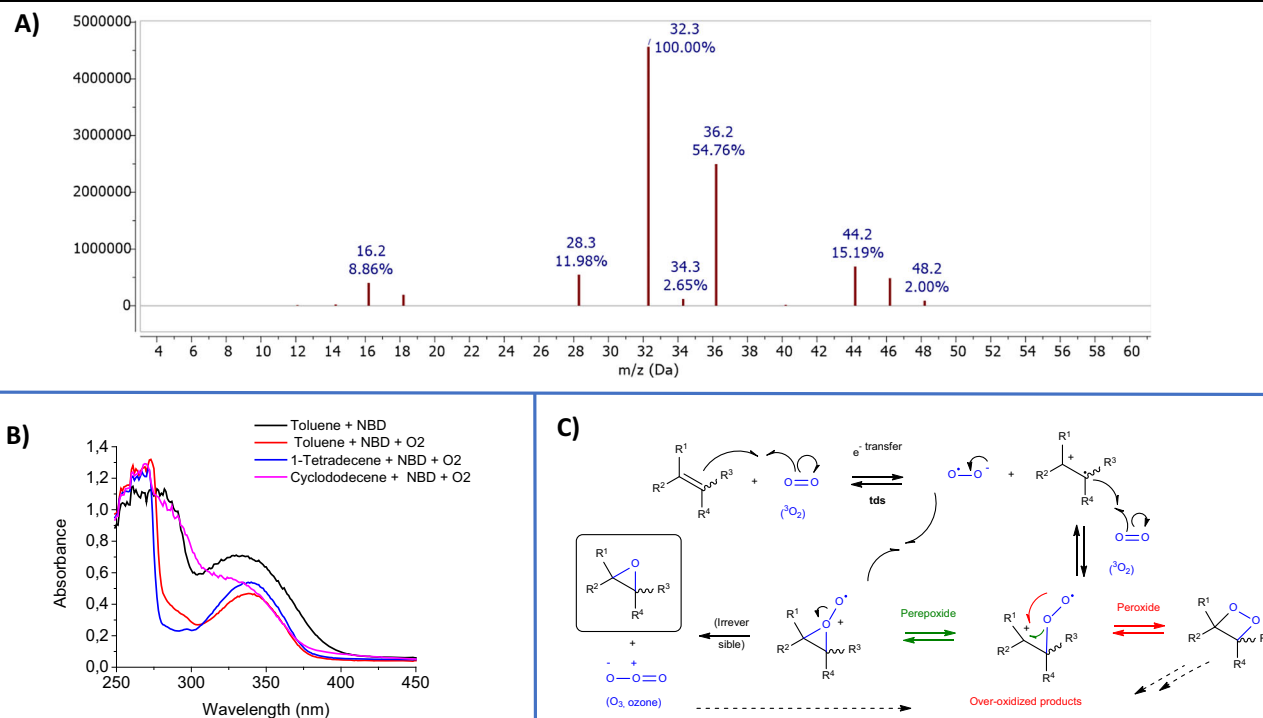


Fig. 6 | Reaction mechanism. A Mass spectrum of the gas phase during the epoxidation reaction of neat tetradecene **1b** under 4 atm of $^{18}\text{O}_2$ in a glass autoclave reactor at 130 °C. **B** Ultraviolet–visible (UV–vis) absorption spectra of 4-chloro-7-

nitrobenzo-2-oxa-1,3-diazole (NBD): in toluene (black line), with O_2 (red line), with O_2 and 1-tetradecene (**1e**, blue line), and with O_2 and cyclododecene (**1f**, pink line) recorded at room temperature. **C** Proposed reaction mechanism.

energy (E_a) of the reaction, using an Arrhenius plot (Fig. S11), which gives $E_a = 74 \text{ kJ}\cdot\text{mol}^{-1}$, within the expected value for a reaction that can proceed at 100 °C¹⁴.

The better reactivity of substituted alkyl alkenes suggests that electron-rich $\text{C}=\text{C}$ double bonds are favored during the epoxidation reaction. Indeed, ^1H and ^{13}C NMR experiments show a shift in the signals associated to the $\text{C}=\text{C}$ bond of 7-tetradecene **1b** in concentrated solutions (Figs. S12 and S13), which indicates a gain of electron density by the alkene after aggregation^{38–40}. This result is confirmed by ultraviolet–visible (UV–vis) absorption spectroscopy analyses (Fig. S14), where a shift in the maximum intensity of the band corresponding to 7-tetradecene **1b**, from 240 to 320 nm, occurs, which corresponds to an energy decrease in the gap between the highest occupied and the lowest unoccupied molecular orbitals (HOMO–LUMO) of 1.2 eV. In other words, it is easier for the alkene to transfer one electron to a suitable electrophile such as O_2 in concentrated, electron-rich solutions (see Fig. S15 for a schematic representation). It is noteworthy to comment that the terminal alkene 1-tetradecene **1e** also aggregates in concentrated solutions and electronically enriches the $\text{C}=\text{C}$ double bonds (Figs. S16–S18), however, which much lesser intensity than the internal counterpart **1b**. Not only terminal alkenes are activated in the presence of internal alkenes (see Figs. 4 and 5), but also the reluctant to epoxidize⁴¹ cyclohexene **1h** (Fig. S19). These results indicate that the more electron density the alkene shows, the better the epoxidation reaction, as it occurs with pre-activated oxidants (i.e., peroxides), and that the concentration of the alkene molecules allows more electron density to be available for O_2 .

The exclusive participation of O_2 during the epoxidation reaction was studied with isotopically labelled and reactivity experiments. When $^{36}\text{O}_2$ instead of $^{32}\text{O}_2$ was used during the epoxidation reaction of **1f**, the corresponding isotopically labelled epoxide product ^{18}O -**2f** was obtained, according to GC–MS (Fig. S20) and Fourier-transformed infrared spectroscopy measurements (FT–IR, Fig. S21), where the expected isotopic mass and infrared shift

were observed. Besides, analysis of the gas phase of the reaction by GC–MS spectroscopy revealed the progressive formation of C^{18}O_2 during reaction, as shown in Fig. 6A. This CO_2 is formed after $\text{C}-\text{C}$ bond breaking and overoxidation of the alkene to carboxylic acids.

Moreover, to confirm that triplet O_2 is involved in the reaction mechanism, we performed the reaction using 7-tetradecene **1b** in the presence of radical scavengers, such as BHT and TEMPO, obtaining 5.4% and 5.6% conversion of alkene, respectively (Fig. S22). The GC–MS analysis of the reaction performed with TEMPO shows the formation of the captured radical alkene by TEMPO. Then, we carried out the experiment using 1-tetradecene and neither the terminal epoxide, the captured radical nor TMPH formation were detected. These results indicate that a simple autooxidation of alkenes by oxygen radicals is not merely in operation, since 1-tetradecene is not reacting in any case, and an alkene radical can be trapped by TEMPO in the presence of triplet O_2 . Nevertheless, we cannot discard an auto-oxidation with simple oxygen radicals.

At this point, three activated O_2 species were considered as potential O donors during the epoxidation reaction: ozone (O_3), singlet oxygen ($^1\text{O}_2$), and superoxide (O_2^-). First, a reactivity test with indigo as a probe molecule was carried out with the alkenes **1f** (internal) and **1e** (terminal) in toluene solution (Fig. S23), in order to seek the formation of O_3 during the epoxidation reaction. In-situ UV–vis results show the disappearance of the indigo absorption band at 604 nm and the appearance of the band at 320 nm, assignable to the oxidation product with O_3 , only with the internal alkene **1f** and not with **1e**, i.e., when the epoxidation reaction occurs. These results suggest the formation of O_3 during the uncatalyzed aerobic epoxidation reaction. The formation of a radical oxygen species in the gas phase⁴² would explain the epoxidation of the terminal alkene **1e** in the two-flasks experiment of Fig. 4, since the terminal alkene can give the epoxide through the allyl mechanism. However, O_3 is prone to break rather than epoxide alkenes, thus O_3 could be considered here as a by-product of the actual epoxidizing species. Indeed, the selectivity to the epoxide product

increases and the conversion slows down in the presence of indigo (Table S5), thus discarding O_3 as the epoxidizing species.

The potential participation of singlet oxygen (1O_2) was studied by reactivity experiments⁴³. To do so, the gas phase of the epoxidation reaction was bubbled into a flask which contained anthracene (0.2 M, $CDCl_3$), with the aiming of forming the corresponding endoperoxide⁴⁴. However, neither the 1H nor the ^{13}C NMR spectrum showed any signal different from those belonging to the starting anthracene (Fig. S24), which discards the formation of significant amounts of singlet oxygen during the epoxidation reaction, hence its possible active role.

In order to determine if the active species was the superoxide radical anion ($O_2^{\cdot-}$), an aromatic derivative described in the literature for quenching this species⁴⁵ was employed as a UV-vis reactive probe: 4-chloro-7-nitrobenzo-2-oxa-1,3-diazole (NBD). As it can be seen in Fig. 6B, only the presence of the more active internal alkene **1f**, and not a terminal alkene, triggered the decomposition of NBD (decrease of the band at 350 nm), thus indicating the formation of the superoxide radical anion ($O_2^{\cdot-}$) during the epoxidation reaction.⁴⁵ The formation of superoxide radical anions ($O_2^{\cdot-}$) during reaction was further checked by employing redox metal salts such as SnO , Fe_2O_3 , or MnO as radical generators, since they are able to react with O_2 and give radical anions and ozone^{46–48}. The results (Table S5) show that the presence of these metal salts significantly increased the conversion of the aerobic reaction of **1b** while keeping a good selectivity for the epoxide **2b**, but also forming the expected overoxidized products at high conversions. The overoxidation of the alkene **1b** was also studied in the presence of different metal oxides (Fig. S25). As it can be observed, after 2-h reaction time, most of the conversions are near complete; however, the selectivity for these metal oxides is, in most cases, lower than when any catalyst is not used for the epoxidation reaction (see for instance V_2O_5 , Fe_2O_3 , and MgO). The other metal oxides tested did not improve the results obtained. For example, the best selectivity for the corresponding epoxide was obtained with MnO_2 , but it also produced a mixture of other overoxidized compounds formed from the rupture of 7-tetradecene **1b**. Furthermore, after a 4-h reaction time, only MoO_3 yields results comparable to those without any catalyst. To confirm whether the activity in the presence of metal oxides follows the mechanism proposed here or the well-known Mars-Van Krevelen mechanism, we performed an additional experiment in which CuO was added under a nitrogen atmosphere. After 4 h of reaction, we obtained a 23% conversion with a selectivity to the epoxide of 42%, 12% to carboxylic acid, 42% to vinyl ketone, and 4% to other compounds. With all these results in hand, we conclude that the addition of metal oxides does not improve the selectivity towards the target epoxide product, and in most cases, it leads to the formation of undesirable compounds. In addition, it is difficult to think that the generation of the superoxide is associated to the metal oxide, moreover considering the that the Mars-Van Krevelen mechanism is under operation. An organic additive such as activated carbon did not promote the epoxidation reaction. Besides, oxoneTM was used as an ozone generator during reaction in stoichiometric amounts with alkenes **1b** and **1e** (Fig. S26), but any epoxidation product could not be found. These results discard ozone as the epoxidizing agent.

With all the above data in mind, the proposed reaction mechanism for the uncatalyzed aerobic epoxidation of alkyl alkenes is shown in Fig. 6C. In accordance with the experimental results, the first step is the one-electron transfer from the alkene to triplet O_2 (3O_2), to generate the corresponding alkene radical cation and the superoxide anion $O_2^{\cdot-}$, respectively. This reaction constitutes the turnover-determining step (tds) of the reaction, fitting well the rate equation obtained through kinetic experiments, where one molecule of each reactant (alkene and O_2) participates. The use of optimum solvents such as perfluorodecaline⁴⁹ to better dissolve the O_2 molecules and increase the yield for epoxides, even in reluctant alkene reactants such as **1d**, confirms the participation of dissolved O_2 in the rds of the

reaction (Fig. S27). Partial O_2 solubility must be directly related to the reaction, thus, the solvent^{50,51}, however, most of the reactions here are performed in neat alkene. It is known that the intermediate alkene radical cation is enough stable and does not rapidly isomerize to contiguous carbon atom positions^{12,44}, in line with the observed epoxidation results.

The radical coupling of a second molecule of 3O_2 to the intermediate alkene radical cation is in principle highly favored, to produce an intermediate zwitterionic radical species which is in equilibrium with two possible *O*-coupled species, the more stable peroxide intermediate (in red) and the less favorable but more reactive perepoxide (in green). All these processes, still in equilibrium, allow the intermediate cationic C–C bond to rotate, thus *cis/trans* isomerization may occur during the epoxidation reaction^{12,14}. To check this, a kinetic experiment with cyclododecene **1f** was performed, showing the enrichment in the thermodynamic more stable *trans* isomer of the epoxide product **2f** during the aerobic epoxidation reaction (Fig. S28), confirming the *cis/trans* isomerization process during reaction.

It has been experimentally and computationally determined^{52,53} that the E_a for the formation of perepoxides from typical alkenes and O_2 is $-80\text{ kJ}\cdot\text{mol}^{-1}$, while the E_a for the formation of the corresponding peroxides is the half, around $-40\text{ kJ}\cdot\text{mol}^{-1}$. These E_a values explain the easy formation of overoxidized products when alkenes are treated with O_2 under inappropriate reaction conditions to generate the epoxides. However, the E_a obtained under the reaction conditions reported here [$E_a = 74\text{ kJ}\cdot\text{mol}^{-1}$ for alkene **1b**, see above] strongly suggests that perepoxide formation takes over and leads to the synthesis of the epoxide by a simple coarctate reaction⁵⁴. The latter occurs after reaction of the perepoxide with the previously generated radical superoxide $O_2^{\cdot-}$, to finally lead to the epoxide product and ozone, the major products experimentally observed during reaction.

The difficulties on finding in the literature any method to prepare perepoxides lead us to perform computational calculations to support the proposed reaction mechanism. These calculations, based on the density functional theory (DFT), were carried out to optimize the molecules involved during the epoxidation reaction of alkene **1b** (see computational details in the SI, and Table S6). The Natural Bond Orbital (NBO) analysis was performed to confirm the electronic distribution of optimized structures (see SI Fig. S29). In case of the perepoxide molecule, the Natural Population Analysis (NPA) indicates that the unpaired electron is largely localized on the terminal oxygen atom (spin density = 0.862), which is consistent with its assignment as the radical center. However, according to the NPA charges, the positive charge is delocalized between this oxygen and the two carbons that form the three-membered ring, since these atoms show partial positive charges. Both radical species shown a delocalization of the unpaired radical between the two atoms that support it, so they show the same value for NPA charge and spin density. Figure 7A shows the better energetic and symmetric compatibility between the highest occupied molecular orbital (HOMO) of the alkene and the lowest unoccupied molecular orbital (LUMO) of O_2 for the more stable β form of triplet 3O_2 , but not for the 3O_2 α form, and also for the singlet 1O_2 , to generate the radical alkene cation and superoxide $O_2^{\cdot-}$ after the electronic transfer from the HOMO of the alkene to the LUMO of either 3O_2 (β form) or 1O_2 . Following this molecular orbital theory approach, Fig. 7B shows that the so-generated alkene cation radical is also able to react with a second molecule of 3O_2 (β form), to generate the corresponding perepoxide, which finally can react with the radical superoxide $O_2^{\cdot-}$ left behind, as shown in Fig. 7C. Indeed, the LUMO and HOMO orbitals of the computed structures match well after interacting each other during the different steps of the reaction (Figs. S29 and S30). These computational results are compatible with the experimental results and strongly support the mechanism proposed involving a perepoxide intermediate. It is noteworthy to comment here that this mechanism is significantly different from other

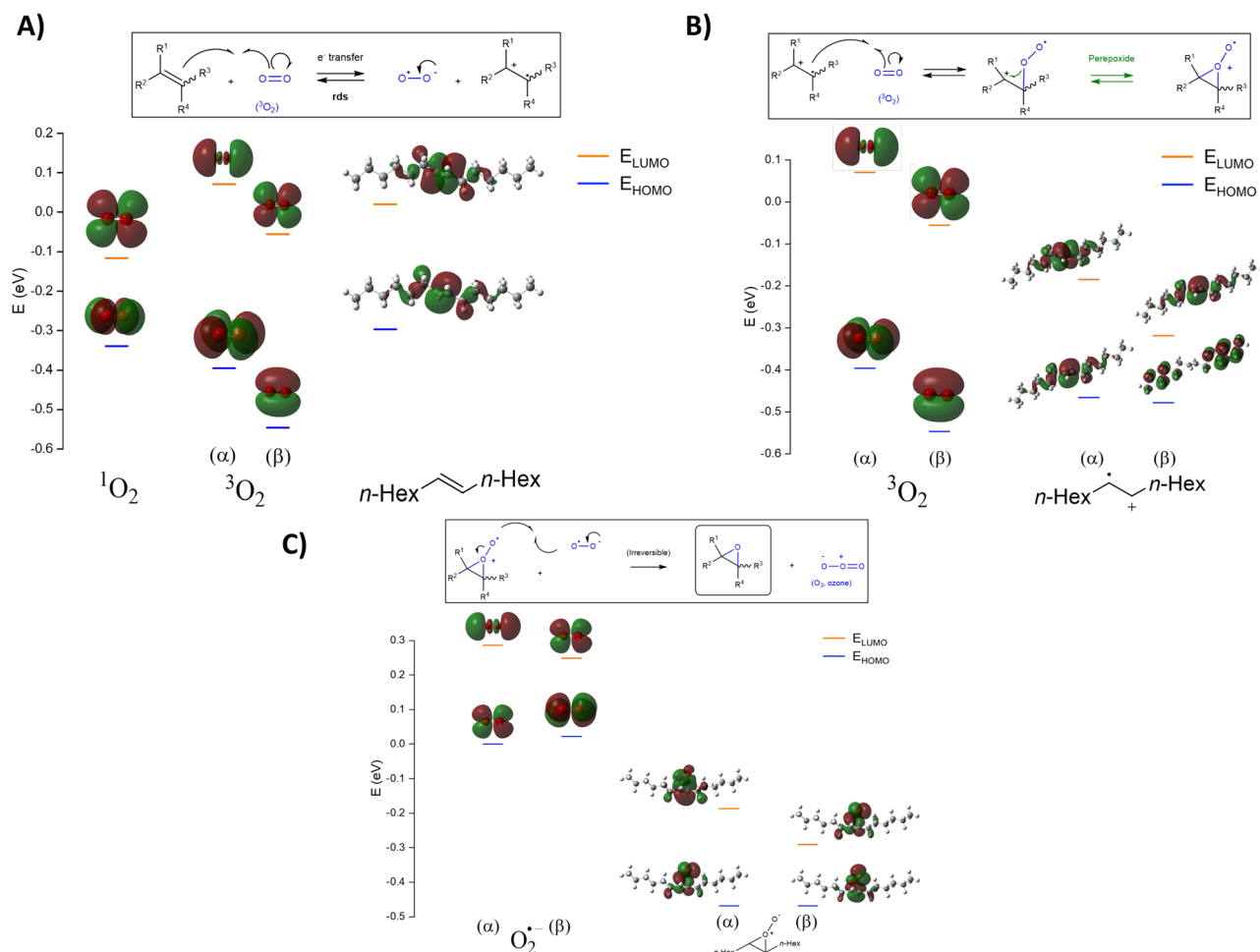


Fig. 7 | DFT calculations. Calculated Gibbs energy profiles at 373.15 K for (A) highest occupied molecular orbital (HOMO) and lowest unoccupied molecular orbital (LUMO) from both singlet (S) and triplet (T) O_2 and alkene **1b**, B HOMO and

LUMO molecular orbitals from triplet oxygen and radical alkene **1b**, and C HOMO and LUMO molecular orbitals from superoxide and peroxide.

proposed for the autooxidation of alkenes, since involves triplet rather than singlet O_2 ^{55,56}, besides to occur in the liquid rather than in the gas phase⁵⁷.

Implications for the ambient oxidation of alkenes

The results shown above infer that alkyl alkenes in contact with the atmosphere will generate the epoxide as the primary product, at least in small amounts. To check this, we examined through GC–MS analysis the open bottles of two representative secondary alkyl alkenes (**1b** and **1f**) available at the laboratory and which do not contain stabilizers such as butylhydroxytoluene (BHT). Apparently, these bottles may have not been stored under inert atmosphere. The results (Fig. S31) show the formation of high amounts of the corresponding epoxides in both cases, up to a 44% of epoxides and overoxidized products. New bottles of the same alkenes were bought and analyzed, showing that the brand-new alkene materials contain some epoxides but in lower extent (Fig. S32). These results demonstrate that secondary alkyl alkenes will generate the epoxide after storage or heating under ambient conditions.

In summary, the aerobic epoxidation of alkyl alkenes can be carried out in good yields and selectivity after heating the neat alkene with O_2 or air in either a pressurized reactor, under O_2 bubbling or just in an open flask. The process does not require any catalyst^{58,59}, solvent nor additive, and can be performed under industrially-feasible reaction conditions, far from flammability points. Fundamental industrial epoxides such as those derived from propylene, cyclic alkenes,

limonene, fatty acids or geraniol can be obtained with this uncatalyzed procedure, which can be engaged in one-pot reactions either with different alkene formations or epoxide transformations. Mechanistic studies reveal that the turnover-limiting step of the epoxidation reaction is the one-electron transfer from the alkene to O_2 , and that peroxide species are potential key intermediates to lead to the epoxide product, and circumvent undesired overoxidation products. The uncatalyzed aerobic epoxidation reaction occurs not only under synthetic conditions but also spontaneously under ambient conditions. These results open a new sustainable pathway for the synthesis of epoxides.

Methods

General

Reagents and solvents were obtained from commercial sources and were used without further purification otherwise indicated. Glassware was dried in an oven at 175 °C before use. Reactions were performed in either house-made glass reactors connected to manometers, round-bottomed flasks or 2.0 ml vials, equipped with a magnetic stirrer. Oxygen or air atmospheres were set after purging three times. ^1H , ^{13}C , and DEPT nuclear magnetic resonance (NMR) spectra were recorded at room temperature on a 400 MHz spectrometer (Bruker Ascend 400) using the appropriate solvent. Infrared spectra were recorded on an Attenuated total reflection (ATR) Fourier transform infrared (FTIR) spectroscopy, performed in a JASCO FT/IR-4700, which was employed to record the IR spectra from 400 to 4000 cm^{-1} of the different solid

catalysts. Gas chromatographic analyses were performed in an instrument (Agilent 8860) equipped with a 30 m × 250 μm × 0.25 μm Agilent HP-50+ capillary column. *N*-dodecane was used as an external standard. GC–MS analyses were performed on a Agilent 8890 N spectrometer equipped with a 30 m × 250 μm × 0.25 μm Agilent HP-5MS UI capillary column and operated under the same conditions. Products were characterized by comparison with the given literature, when possible. Absorption and emission ultraviolet–visible spectroscopy measurements were performed on the same samples than that for mass determination, using an UV–vis (UV0811M209, Varian) and a LP S–220B spectrophotometer (Photon Technology International, equipped with 75 W Xe lamp), respectively. DFT electronic structure calculations were performed using the software Gaussian 09 with the M06-2× coupled with the 6–31+G(3df,2p) basis set. Geometries of reactants, intermediates and products were optimized by calculating vibration frequencies to confirm that an energy minimum was found. A Natural Bond Orbital (NBO) analysis was performed to obtain the Natural Population Analysis (NPA) charges and NPA spin densities. Graphics were represented in the Excel™ program and the error bars represent a particular confidence interval, in this case a 95% confidence.

Reaction procedures

Typical reaction procedure for pressurized reactors. In a 7.5 mL autoclave equipped with a magnetic bar and a manometer, 0.5 mmol of the corresponding alkene **1b–1t** is added, three purges are made with oxygen and, then, the reactor is charged at 3–5 bar of oxygen pressure, heated at 130 °C for 1.5 h, and the reaction followed by GC until its complete conversion. Afterwards, if required, the mixture was purified by flash chromatography using as an eluent a hexane: ethyl acetate mixture (typically 10:1, *v:v*), obtaining the pure epoxide with the corresponding yield (Figs. 2 and 3).

Typical reaction procedure for O₂ bubbling. In a 25 mL round-bottomed flask stoppered with a septum, 5 mmol of the corresponding alkene **1b**, **1f**, **1n**, or **1p** are introduced and heated to 130 °C, and a capillary with an oxygen flow of 1 mL·min^{−1} is introduced to the bottom of the flask, so that a slight bubbling is produced in the starting alkene product. An outlet orifice is let to avoid pressure inside the flask. The reaction is followed by drawing aliquots periodically and measured them on the GC, until maximum conversion. Once the reaction is finished, the mixture is purified (if required) by flash chromatography using as an eluent a hexane: ethyl acetate mixture (typically 10:1, *v:v*), to obtain the pure epoxide with the corresponding yield (Figs. 2 and 3).

Typical reaction procedure for open flasks. In a 10 mL round-bottomed flask equipped with a magnetic bar, 5 mmol of the corresponding alkene **1b**, **1e**, **1f**, **1g**, **1p**, or **1u–1y** is introduced, and a reflux condenser open to the air is adapted. The mixture is heated at 150 °C for 16–20 h, aliquots are periodically removed and measured by GC, in order to follow the reaction progress until it reaches a maximum conversion. Once finished, the mixture is purified by flash chromatography (if required) using as an eluent a hexane: ethyl acetate mixture (typically 10:1, *v:v*), to obtain the pure epoxide with the corresponding yield (Figs. 2 and 3).

A representative one-pot reaction. In a round-bottomed flask equipped with a magnetic bar, the corresponding terminal alkene (1 mmol) and the Grubbs' 1st generation catalyst (5 mol%) were added and stirred at 90 °C for 18 h. Then, the flask was connected to a reflux condenser and heated at 130 °C for 1.5 h. The reaction was monitored after taking out and measuring aliquots by GC, until maximum conversion. Once the reaction is finished, the mixture is purified by flash chromatography using as an eluent a hexane: ethyl acetate mixture (10:1, *v:v*), to obtain the pure epoxide **2aa** in 43% yield (Fig. 5A).

Computational details

DFT electronic structure calculations were performed using the software Gaussian 09 with the M06-2× coupled with the 6–31+G(3df,2p) basis set. Geometries of reactants, radical intermediates, and products were optimized by calculating vibration frequencies at 373.15 K of temperature to confirm that it is a energy minimum. A Natural Bond Orbital (NBO) analysis was performed to obtain the Natural Population Analysis (NPA) charges and NPA spin densities.

Data availability

The datasets generated during and/or analysed during the current study are included in this published article (and its supplementary information files) or available from the corresponding author on request. Datasets could be also deposited in public repositories of the UPV and CSIC. Source data are provided with this paper.

References

1. Meng, Y. et al. The lord of the chemical rings: catalytic synthesis of important industrial epoxide compounds. *Catalysts* **11**, 765 (2021).
2. Berndt, T. & Böge, O. Gas-phase epoxidation of propylene and ethylene. *Ind. Eng. Chem. Res.* **44**, 645–650 (2005).
3. Nishiyama, Y., Nakagawa, Y. & Mizuno, N. High turnover numbers for the catalytic selective epoxidation of alkenes with 1 atm of molecular oxygen. *Angew. Chem. Int. Ed.* **40**, 3639–3641 (2001).
4. Aprile, C., Corma, A., Domine, M. E., Garcia, H. & Mitchell, C. A cascade aerobic epoxidation of alkenes over Au/CeO₂ and Ti-mesoporous Material by “In situ” Formed Peroxides. *J. Catal.* **264**, 44–53 (2009).
5. Pattisson, S. et al. Tuning graphitic oxide for initiator- and metal-free aerobic epoxidation of linear alkenes. *Nat. Commun.* **7**, 12855 (2016).
6. Stamoulis, A. G., Bruns, D. L. & Stahl, S. S. Optimizing the synthetic potential of O₂: implications of overpotential in homogeneous aerobic oxidation catalysis. *J. Am. Chem. Soc.* **145**, 17515–17526 (2023).
7. Liu, H. et al. Modulating charges of dual sites in multivariate metal-organic frameworks for boosting selective aerobic epoxidation of alkenes. *J. Am. Chem. Soc.* **145**, 11085–11096 (2023).
8. Blanckenberg, A. & Malgas-Enus, R. Olefin epoxidation with metal-based nanocatalysts. *Catal. Rev.* **61**, 27–83 (2019).
9. Lu, X.-H. et al. Non-metallic ketone compounds catalyzed selective epoxidation of styrene with dry air. *Catal. Lett.* **132**, 487–491 (2009).
10. Hadian-Dehkordi, L. & Hosseini-Monfared, H. Enantioselective aerobic oxidation of olefins by magnetite nanoparticles at room temperature: a chiral carboxylic acid strategy. *Green. Chem.* **18**, 497–507 (2016).
11. Sanz-Navarro, S. et al. Radical α-alkylation of ketones with unactivated alkenes under catalytic and sustainable industrial conditions. *Appl. Catal. A* **613**, 118021 (2021).
12. Correa, P. E., Hardy, G. & Riley, D. P. Selective autoxidation of electron-rich substrates under elevated oxygen pressures. *J. Org. Chem.* **53**, 1695–1702 (1988).
13. Mahajani, S. M., Sharma, M. M. & Sridhar, T. Uncatalysed oxidation of cyclohexene. *Chem. Eng. Sci.* **54**, 3967–3976 (1999).
14. Mahajan, S. S., Sharma, M. M. & Sridhar, T. Uncatalyzed liquid-phase oxidation of cyclododecene with molecular oxygen. *Ind. Eng. Chem. Res.* **43**, 3289–3296 (2004).
15. Gonzalez-de-Castro, A. & Xiao, J. Green and efficient: iron-catalyzed selective oxidation of olefins to carbonyls with O₂. *J. Am. Chem. Soc.* **137**, 8206–8218 (2015).
16. Soler, J., Gergel, S., Klaus, C., Hammer, S. C. & Garcia-Borràs, M. Enzymatic control over reactive intermediates enables direct oxidation of alkenes to carbonyls by a P450 iron-oxo species. *J. Am. Chem. Soc.* **144**, 15954–15968 (2022).

17. Mill, T. & Hendry, D. G. Chapter 1 Kinetics and mechanisms of free radical oxidation of alkanes and olefins in the liquid phase. In *Liquid-Phase Oxidation* (eds. Bamford, C. H. et al.) Vol. **16**, 1–87 (Elsevier, 1980).
18. Van Sickle, D. E., Mayo, F. R., Arluck, R. M. & Syz, M. G. Oxidations of acyclic alkenes. *J. Am. Chem. Soc.* **89**, 967–977 (1967).
19. Diaz, R. R., Selby, K. & Waddington, D. J. Reactions of oxygenated radicals in the gas phase. Part I. Reaction of peracetyl radicals and but-2-Ene. *J. Chem. Soc. Perkin. Trans.* **2**, 758–763 (1975).
20. Suprun, W. Y. & Opeida, J. Studies on the autoxidation of aryl alkenes. *Chem. Eng. Technol.* **29**, 1253–1261 (2006).
21. Metelitsa, D. I. Reaction mechanisms of the direct epoxidation of alkenes in the liquid phase. *Russ. Chem. Rev.* **41**, 807 (1972).
22. Filippova, T. V. & Blyumberg, E. A. Mechanism of the epoxidation of alkenes by molecular oxygen. *Russ. Chem. Rev.* **51**, 582 (1982).
23. Sanz-Navarro, S. et al. Parts-per-million of ruthenium catalyze the selective chain-walking reaction of terminal alkenes. *Nat. Commun.* **13**, 2831 (2022).
24. Kumar, V. & Chimni, S. S. Metal-free ring-opening of epoxides. *ChemistrySelect* **8**, e202301963 (2023).
25. Cvetanović, R. J. Molecular rearrangements in the reactions of oxygen atoms with olefins. *Can. J. Chem.* **36**, 623–634 (1958).
26. Van Sickle, D. E., Mayo, F. R. & Arluck, R. M. Liquid-phase oxidations of cyclic alkenes. *J. Am. Chem. Soc.* **87**, 4824–4832 (1965).
27. Maranzana, A., Ghigo, G. & Tonachini, G. Mechanistic significance of peroxide trapping experiments, with epoxide detection, in 1Δg dioxygen reactions with alkenes. *J. Org. Chem.* **68**, 3125–3129 (2003).
28. Moriai, T., Tsukamoto, T., Tanabe, M., Kambe, T. & Yamamoto, K. Selective hydroperoxylation of olefins realized by a coinage multimetallic 1-nanometer catalyst. *Angew. Chem. Int. Ed.* **59**, 23051–23055 (2020).
29. Leach, A. G., Houk, K. N. & Foote, C. S. Theoretical prediction of a peroxide intermediate for the reaction of singlet oxygen with trans-cyclooctene contrasts with the two-step no-intermediate ene reaction for acyclic alkenes. *J. Org. Chem.* **73**, 8511–8519 (2008).
30. Alshammari, H., Miedziak, P. J., Knight, D. W., Willock, D. J. & Hutchings, G. J. The effect of ring size on the selective oxidation of cycloalkenes using supported metal catalysts. *Catal. Sci. Technol.* **3**, 1531–1539 (2013).
31. Wu, Y. et al. Sustainable and practical access to epoxides: metal-free aerobic epoxidation of olefins mediated by peroxy radical generated in situ. *ACS Sustain. Chem. Eng.* **8**, 1178–1184 (2020).
32. Keleş, E. & Hazer, B. Autooxidized polyunsaturated oils/oily acids: post-it applications and reactions with Fe(III) and adhesion properties. *Macromol. Symp.* **269**, 154–160 (2008).
33. Westerman, C. R., McGill, B. C. & Wilker, J. J. Sustainably sourced components to generate high-strength adhesives. *Nature* **621**, 306–311 (2023).
34. Garnes-Portolés, F. et al. Regioirregular and catalytic Mizoroki-Heck reactions. *Nat. Catal.* **4**, 293–303 (2021).
35. Garnes-Portolés, F., Sánchez-Quesada, J., Espinós-Ferri, E. & Leyva-Pérez, A. Synthesis of dehydromusccone by an alkene metathesis macrocyclization reaction at 0.2 M concentration. *Synlett* **33**, 1933–1937 (2022).
36. Garhwal, S., Kaushansky, A., Fridman, N. & de Ruiter, G. Part per million levels of an anionic iron hydride complex catalyzes selective alkene isomerization via two-state reactivity. *Chem. Catal.* **1**, 631–647 (2021).
37. Sato, T., Hamada, Y., Sumikawa, M., Araki, S. & Yamamoto, H. Solubility of oxygen in organic solvents and calculation of the Hansen solubility parameters of oxygen. *Ind. Eng. Chem. Res.* **53**, 19331–19337 (2014).
38. Van den Ven, L. J. M., De Haan, J. W. & Bucinska, A. Conformational equilibria of normal alkanes, 1-alkenes, and some (E)- and (Z)-2-alkenes in neat liquids and in some selected solvents. A carbon-13 nuclear magnetic resonance study. *J. Phys. Chem.* **86**, 2516–2522 (1982).
39. Li, M.-Y. et al. Solvent-free and catalyst-free direct alkylation of alkenes. *Green. Chem.* **25**, 7073–7078 (2023).
40. Li, M.-Y. et al. Aggregation-enabled alkene insertion into carbon-halogen bonds. *Aggregate* **4**, e346 (2023).
41. Mitsudome, T., Mizumoto, K., Mizugaki, T., Jitsukawa, K. & Kaneda, K. Wacker-type oxidation of internal olefins using a PdCl₂/N,N-dimethylacetamide catalyst system under copper-free reaction conditions. *Angew. Chem. Int. Ed.* **49**, 1238–1240 (2010).
42. Williams, P. J. H. et al. New approach to the detection of short-lived radical intermediates. *J. Am. Chem. Soc.* **144**, 15969–15976 (2022).
43. Clennan, E. L. & Pace, A. Advances in singlet oxygen chemistry. *Tetrahedron* **61**, 6665–6691 (2005).
44. Díaz-Urbe, C. E., Vallejo-Lozada, W. A. & Martínez-Ortega, F. Photooxidation of anthracene under visible light with metallo-carboxyphenylporphyrins. *Rev. Fac. Ing. Univ. Antioquia* **73**, 225–230 (2014).
45. Olojo, R. O., Xia, R. H. & Abramson, J. J. Spectrophotometric and fluorometric assay of superoxide ion using 4-Chloro-7-nitrobenzo-2-oxa-1,3-diazole. *Anal. Biochem.* **339**, 338–344 (2005).
46. Li, M.-S. et al. Catalyst-free direct difunctionalization of alkenes with H-phosphine oxides and dioxygen: a facile and green approach to β-hydroxyphosphine oxides. *Tetrahedron Lett.* **57**, 2642–2646 (2016).
47. Heisig, C., Zhang, W. & Oyama, S. T. Decomposition of ozone using carbon-supported metal oxide catalysts. *Appl. Catal. B* **14**, 117–129 (1997).
48. Li, J. et al. Low pressure induced porous nanorods of ceria with high reducibility and large oxygen storage capacity: synthesis and catalytic applications. *J. Mater. Chem. A* **2**, 16459–16466 (2014).
49. Riess, J. G. Understanding the fundamentals of perfluorocarbons and perfluorocarbon emulsions relevant to in vivo oxygen delivery. *Artif. Cells, Blood Substit., Biotechnol.* **33**, 47–63 (2005).
50. Zhang, S., Song, P. & Li, S. Application of N-dodecane as an oxygen vector to enhance the activity of fumarase in recombinant *Escherichia coli*: role of intracellular microenvironment. *Braz. J. Microbiol.* **49**, 662–667 (2018).
51. Wentzel, B. B., Alsters, P. L., Feiters, M. C. & Nolte, R. J. M. Mechanistic studies on the Mukaiyama epoxidation. *J. Org. Chem.* **69**, 3453–3464 (2004).
52. Yamaguchi, K., Yabushita, S., Fueno, T., Kato, S. & Morokuma, K. Geometry optimization of the ring-opened oxirane diradical: mechanism of the addition reaction of the triplet oxygen atom to olefins. *Chem. Phys. Lett.* **70**, 27–30 (1980).
53. Malek, B. et al. Probing the transition state-to-intermediate continuum: mechanistic distinction between a dry versus wet peroxide in the singlet oxygen “Ene” reaction at the air-water interface. *Langmuir* **38**, 6036–6048 (2022).
54. Herges, R. Coarctate and pseudocoarctate reactions: stereochemical rules. *J. Org. Chem.* **80**, 11869–11876 (2015).
55. Dias, A. M. A., Freire, M., Coutinho, J. A. P. & Marrucho, I. M. Solubility of oxygen in liquid perfluorocarbons. *Fluid Phase Equilib.* **222–223**, 325–330 (2004).
56. Rao, T. S. S. & Awasthi, S. Oxidation of olefins. *J. Indian Chem. Soc.* **84**, 902–913 (2007).
57. Berndt, T. & Böge, O. Catalyst-free gas-phase epoxidation of alkenes. *Chem. Lett.* **34**, 584–585 (2005).
58. Teržan, J., Huš, M., Likozar, B. & Djinović, P. Propylene epoxidation using molecular oxygen over copper- and silver-based catalysts: a review. *ACS Catal.* **10**, 13415–13436 (2020).

59. Kiani, D. & Wachs, I. E. Practical considerations for understanding surface reaction mechanisms involved in heterogeneous catalysis. *ACS Catal.* **14**, 16770–16784 (2024).

Acknowledgements

This work is part of the project PID2023-148441NB-I00 funded by MCIN/AEI/10.13039/501100011033MICIIN (Spain). Financial support by Severo Ochoa centre of excellence program (CEX2021-001230-S) is gratefully acknowledged. The work has also been funded by Generalitat Valenciana (Prometeo Grupos de Investigación de Excelencia PROMETEU/2021/054, and INNEST/2022/20 from Agència Valenciana de la Innovació). Funding for open access charge: Universitat Politècnica de València. S.R.-N. thanks Agència Valenciana de la Innovació for a contract. J.O.-M. thanks the MICIIN for the concession of the Ramón y Cajal contract RYC2022-036154-I (funded by MCIN/AEI/10.13039/501100011033). S.H.-A. and F.G.-P. thanks ITQ for the concession of a contract. We thank Dr Mercedes Boronat and Miguel Ródenas Espada for unvaluable helping during the DFT calculations.

Author contributions

S.H.-A. performed the epoxidation reactions, the one-pot isomerization-epoxidation reactions, DFT calculations, and mechanistic experiments. F.G.-P. discovered the uncatalyzed reaction, performed the epoxidation reactions and the one-pot metathesis-epoxidation reactions, and mechanistic experiments. S.R.-N. performed epoxidation reactions, the one-pot epoxidation-epoxide transformations, and mechanistic experiments. J.O.-M. epoxidation reactions and mechanistic experiments, and supervised to S.H.-A. A.L.-P. designed the experiments and supervised the whole work. The manuscript has been written with contributions from all authors, which also interpreted all the experimental part.

Competing interests

A Spanish patent (number P202430625) covering the uncatalyzed epoxidation reaction of alkenes has been filled, appearing as co-inventors S.H.-A., F.G.-P., J.O.-M., and A.L.-P. Another Spanish patent (number P202430884) covering the Ru-catalyzed one-pot isomerization-epoxidation reaction of alkenes has been filled, appearing as co-inventors S.H.-A., S.R.-N., and A.L.-P.

Additional information

Supplementary information The online version contains supplementary material available at <https://doi.org/10.1038/s41467-025-61711-3>.

Correspondence and requests for materials should be addressed to Judit Oliver-Meseguer or Antonio Leyva-Pérez.

Peer review information *Nature Communications* thanks Landong Li, and the other, anonymous, reviewers for their contribution to the peer review of this work. A peer review file is available.

Reprints and permissions information is available at <http://www.nature.com/reprints>

Publisher's note Springer Nature remains neutral with regard to jurisdictional claims in published maps and institutional affiliations.

Open Access This article is licensed under a Creative Commons Attribution-NonCommercial-NoDerivatives 4.0 International License, which permits any non-commercial use, sharing, distribution and reproduction in any medium or format, as long as you give appropriate credit to the original author(s) and the source, provide a link to the Creative Commons licence, and indicate if you modified the licensed material. You do not have permission under this licence to share adapted material derived from this article or parts of it. The images or other third party material in this article are included in the article's Creative Commons licence, unless indicated otherwise in a credit line to the material. If material is not included in the article's Creative Commons licence and your intended use is not permitted by statutory regulation or exceeds the permitted use, you will need to obtain permission directly from the copyright holder. To view a copy of this licence, visit <http://creativecommons.org/licenses/by-nc-nd/4.0/>.

© The Author(s) 2025